

Technical University of Denmark



Inductance mode characteristics of a ceramic YBa₂Cu₃O_{7-x} radio-frequency superconducting quantum interference device at 77 K

Il'ichev, E. V.; Andreev, A. V.; Jacobsen, Claus Schelde

Published in:
Journal of Applied Physics

Link to article, DOI:
[10.1063/1.354537](https://doi.org/10.1063/1.354537)

Publication date:
1993

Document Version
Publisher's PDF, also known as Version of record

[Link back to DTU Orbit](#)

Citation (APA):
Il'ichev, E. V., Andreev, A. V., & Jacobsen, C. S. (1993). Inductance mode characteristics of a ceramic YBa₂Cu₃O_{7-x} radio-frequency superconducting quantum interference device at 77 K. *Journal of Applied Physics*, 74(5), 3572-3575. DOI: 10.1063/1.354537

DTU Library

Technical Information Center of Denmark

General rights

Copyright and moral rights for the publications made accessible in the public portal are retained by the authors and/or other copyright owners and it is a condition of accessing publications that users recognise and abide by the legal requirements associated with these rights.

- Users may download and print one copy of any publication from the public portal for the purpose of private study or research.
- You may not further distribute the material or use it for any profit-making activity or commercial gain
- You may freely distribute the URL identifying the publication in the public portal

If you believe that this document breaches copyright please contact us providing details, and we will remove access to the work immediately and investigate your claim.

Inductance mode characteristics of a ceramic $\text{YBa}_2\text{Cu}_3\text{O}_{7-x}$ radio-frequency superconducting quantum interference device at 77 K

E. V. Il'ichev,^{a)} A. V. Andreev,^{b)} and C. S. Jacobsen
Physics Department, The Technical University of Denmark, DK-2800 Lyngby, Denmark

(Received 23 March 1993; accepted for publication 10 May 1993)

Experimental results on some radio-frequency superconducting quantum interference device (rf-SQUID) signal properties are presented. The quantum interferometer was made of ceramic $\text{YBa}_2\text{Cu}_3\text{O}_{7-x}$ and was due to a low critical current operated in the inductance or nonhysteretic mode. With bias current as reference, amplitude variation, and phase shift of the voltage over the tank circuit coupled to the SQUID were measured simultaneously. It is shown that there is qualitative agreement between calculations based on the resistivity shunted junction model and the data. Moreover, using phase detection, signal instabilities predicted for the rf-SQUID inductance mode were observed. These signal instabilities may be exploited to enhance the transfer coefficient for measured flux-to-output signal.

I. INTRODUCTION

With the discovery of the high-critical-temperature (HCT) superconductors, it became of great interest to explore their applicability in superconducting quantum interference devices (SQUIDS). It was clear that if just some of the extreme sensitivity to magnetic flux known from low-critical-temperature SQUIDS could be preserved at an operation temperature of, for example, 77 K, the range of useful applications for SQUIDS could be drastically widened. As is well known, both promising radio-frequency (rf)^{1,2} and direct-current (dc)³ SQUIDS have now been demonstrated for 77 K operation. This success suggests the importance of exploring all aspects of HCT-SQUID fabrication and operation. In this article we report on some results on a rf SQUID made of ceramic $\text{YBa}_2\text{Cu}_3\text{O}_{7-x}$ (YBCO), and operated in the not traditionally used inductance (nonhysteretic) mode.

A rf SQUID basically consists of a superconducting loop with a single weak link (the quantum interferometer) inductively coupled to a radio-frequency-biased tank circuit (resonant LC circuit). A flux ϕ_x applied to the loop changes the average value of the phase shift across the weak link, which via the Josephson equations corresponds to an effective change in the interaction between loop and tank circuit. Thus, a flux change can be detected as changes in amplitude and phase of the voltage across the tank circuit. An important parameter which characterizes the SQUID operation is $\beta = 2\pi LI_C/\Phi_0$, where L is the SQUID loop inductance, I_C is the critical current of the weak link, and Φ_0 is the flux quantum.⁴ If $\beta < 1$ the mode of operation is inductive or nonhysteretic (the total loop flux versus applied flux characteristic shows no jumps). If $\beta > 1$, the mode of operation is dissipative or hysteretic with jumps occurring. Usually, the latter mode is employed, because it has the higher flux to voltage transfer

coefficient. However, under certain circumstances the transfer coefficient in the dispersive mode may be enhanced tremendously,^{5,6} thus making such operation worth exploring in detail.

In the nonhysteretic mode the response can be considered due to a parametric inductance.⁴ The effective tank-circuit inductance becomes simply a periodic function of the applied magnetic flux ϕ_x because of the coupling to the SQUID loop. Therefore, the resonance frequency ω_0 of the tank-circuit SQUID system also becomes a function of ϕ_x . According to Ref. 5 it is useful to introduce two transfer coefficients for amplitude and phase, respectively,

$$\eta_a = \left| \frac{\partial V_a}{\partial \phi_x} \right|, \quad \eta_\theta = V_a \left| \frac{\partial \theta}{\partial \phi_x} \right|. \quad (1)$$

Calculations based on the resistively shunted junction (RSJ) model⁵ show that the fundamental thermal noise referred to the input as a flux noise spectral density has the following dependencies on the tank-circuit properties and bias frequency (bias current constant):

$$(S_\varphi)_a = \text{const} \{ [(2Q)^{-2} + \xi^2]/\xi^2 \}^{1/2}, \\ (S_\varphi)_\theta = \text{const} \{ [(2Q)^{-2} + \xi^2]/(2Q)^{-2} \}, \quad (2)$$

for amplitude and phase detection, respectively. In these expressions, $\xi = (\omega - \omega_0)/\omega_0$ is the detuning, ω being the actual pump or bias frequency, while Q is the quality factor of the tank circuit. It follows that optimum sensitivity for amplitude detection is obtained under the condition $\xi > (2Q)^{-1}$, i.e., far from the resonance frequency, while optimum sensitivity for phase detection is obtained under the condition $\xi < (2Q)^{-1}$, i.e., in resonance. Because the signal level is low away from resonance, this suggests that amplitude detection is unfavorable, or rather it requires a very low amplifier noise.

Now let us qualitatively discuss what happens when the bias frequency is changed through the resonance in the inductance mode. We assume that the bias current amplitude and the external magnetic flux at the SQUID loop are kept constant. Because of the resonant properties of the tank circuit the flux, ϕ_{rf} , coupled to the SQUID loop from

^{a)}Permanent address: Institute of Problems of the Technology of Microelectronics and Highly Pure Materials, Russian Academy of Sciences, Chernogolovka, Moscow district 142432, Russia.

^{b)}Permanent address: Institute of Radio Engineering and Electronics, Russian Academy of Sciences, Moscow 103907, Russia.

the tank circuit will change with bias frequency, and due to the strong nonlinearity of the SQUID the resonance frequency itself becomes frequency dependent in a nonmonotonic way. As shown in Ref. 5 the shape of the frequency-dependent response can be quite unusual. As a consequence the whole resonance curve will also depend (periodically) on the applied dc flux, and for certain parameter values the instabilities may occur (i.e., the resonance curve contains points of infinite slope or is even multivalued). It follows from calculations⁵ that this requires two conditions to be fulfilled: $k^2 Q \beta > 1$ and $\phi_{rf} > \Phi_0$. k is the coupling coefficient given by $k = M / \sqrt{L L_T}$, where M is the mutual inductance, and L_T is the tank circuit inductance.

If the resonance curve has multivalued regions, an arbitrarily small change in the external flux can cause a finite change in the response. So, in a restricted region of parameter space, the transfer coefficients η_a and η_ϕ may become very large.

Investigations of Nb SQUIDS with point contacts of high quality, conducted at $T = 4.2$ K,⁶ have confirmed the predictions.⁵ Moreover, due to the high transfer coefficients it appeared possible to reach levels of sensitivity known from dc-SQUIDS. For HCT rf SQUIDS the inductance mode has already been demonstrated,¹² however, investigation of the signal properties was not carried out. Hence, it is the goal of the present work to address the following two connected questions: (i) Do the predictions of Ref. 5 based on the RSJ model apply for a rf SQUID with a weak link of macroscopic dimensions? (ii) If so, is it possible even at 77 K to find features in the signals related to the instabilities discussed above?

II. EXPERIMENT

The samples were made from an $\text{YBa}_2\text{Cu}_3\text{O}_{7-x}$ ceramic of high mechanical strength, but moderate critical-current density ($50\text{--}100$ A/cm² at 77 K). The superconducting transition temperature is 90 K with a width of the transition of order 2 K. The rf SQUID is made out of a disk 2 mm in diameter and 2 mm thick. A 0.4 mm hole is drilled in the center, while in the lateral surface a slit is cut leaving a bridge with minimum dimensions of about 20–30 μm (see Fig. 1). A coil wound of 20- μm -diam Cu wire is inserted in the hole. This coil is part of the tank circuit, which has its resonance frequency near 30 MHz and an effective Q of 30. The schematics of the measuring system is shown in Fig. 2. The rf generator determines the frequency of the bias signal, while the amplitude is set by attenuators. The preamplified tank-circuit voltage and a reference voltage is fed to a vector voltmeter. The vector voltmeter transforms the high-frequency signals into 20 kHz signals without losing information about the amplitudes and the relative phase. The 20 kHz signals are then demodulated by a two-phase lock-in amplifier, allowing us to track simultaneously amplitude and phase as function of applied magnetic flux. The applied flux is generated by a dc

INTERFEROMETER DESIGN

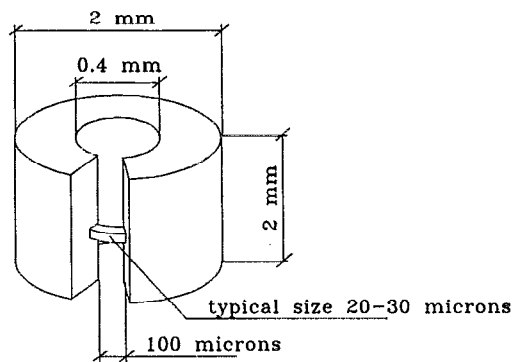


FIG. 1. Schematic drawing of the ceramic rf SQUID.

generator by superimposing a dc current onto the rf current in the tank-circuit coil. The data are registered by a two-channel X-Y recorder.

All the measurements were carried out in liquid nitrogen ($T = 77$ K). The SQUID was magnetically shielded with a 10 cm $\text{YBa}_2\text{Cu}_3\text{O}_{7-x}$ ceramic tube of internal diameter 12 mm and external diameter 18 mm.

III. RESULTS

An example of simultaneous registration of amplitude and phase is shown in Fig. 3. The signal period is consistent with the value of Φ_0 and the geometry of the coil and SQUID and can then be used for a precise determination of M through $M \Delta I_{dc} = \Phi_0$, where ΔI_{dc} is the observed period in the signal measured as a current increment. Now the dependence on the bias frequency can be mapped out.

Initially the maximum SQUID response was found with varying bias current and frequency for phase and amplitude detection, respectively. As might be expected bias current and frequency for optimum response were found to be different in the two cases. The flux modulation corresponding to the bias current can be estimated. If the amplitude of the rf flux is called ϕ_{rf} , then assuming that M is

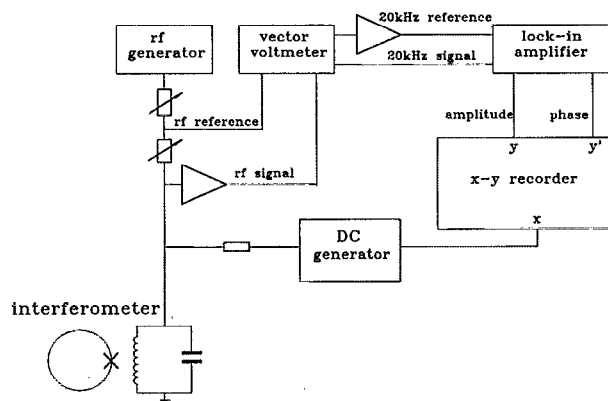


FIG. 2. Block diagram of the experimental setup.

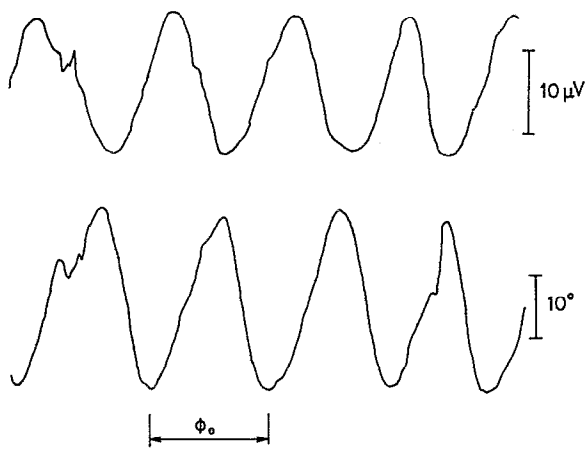


FIG. 3. An example of simultaneous phase and amplitude detection of rf SQUID response.

frequency independent, we have $\phi_{rf} = I_{rf}/M = \Delta I_{dc} \Phi_0 / I_{rf}$, where I_{rf} is the amplitude of the circuit rf current. Since I_{rf} can be estimated from the bias current, the frequency, and the circuit parameters, it is possible to determine the optimum rf-flux amplitude for the two detection modes, respectively. These were found to be $\phi_{rf} \approx \Phi_0/2$ for phase detection and $\phi_{rf} \approx 3\Phi_0/2$ for amplitude detection.

The frequency dependence of the optimum SQUID response is shown in Fig. 4 for phase detection and in Fig. 5 for amplitude detection. For phase detection the maximum response is observed near resonance for the tank circuit (28.5 MHz) as expected from the model. For amplitude detection a distinct asymmetry is seen, but it is evident that a dip in the response is found near the tank-circuit resonance. This is also in accord with the model. Thus, we may conclude that the SQUID is basically operating in the inductance mode.

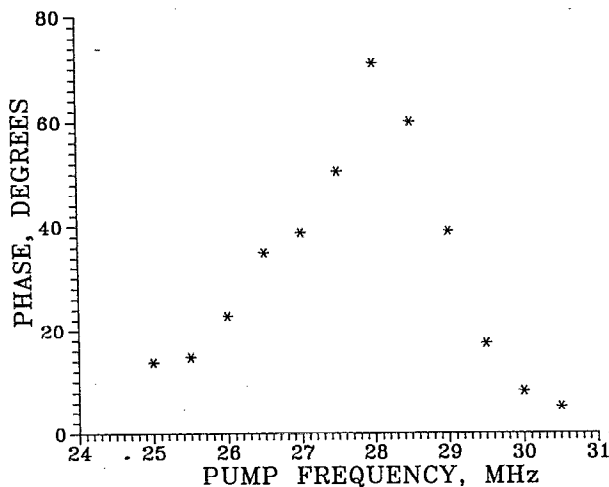


FIG. 4. Frequency dependence of the SQUID response for constant-bias current, measured as peak-to-peak change in phase of tank-circuit voltage. The bias current has been selected to have $\phi_{rf} \approx \Phi_0/2$ in resonance (optimum response).

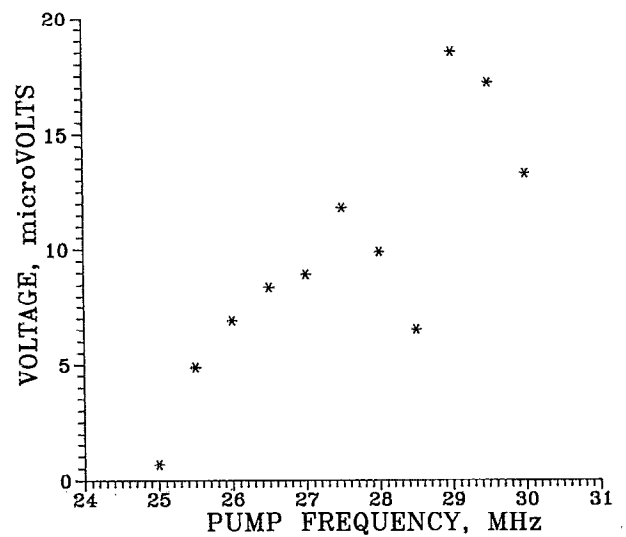


FIG. 5. Frequency dependence of the SQUID response for constant-bias current, measured as peak-to-peak change in amplitude of tank-circuit voltage. The bias current has been selected to have $\phi_{rf} \approx 3\Phi_0/2$ in resonance (optimum response).

It should be noted that the resonance frequency of the coupled system shifts about 0.5 MHz with the change in ϕ_{rf} (see Figs. 4 and 5). This shift is again due to the nonlinearities in the SQUID and the observation suggests that it should be possible to see signatures of the instabilities described in the introduction if ϕ_{rf} is further increased.

Simultaneously obtained traces of phase and amplitude detection are shown in Fig. 6 at a bias frequency of 28.5 MHz, and for power levels with ϕ_{rf} around $5\phi_0$. The level for the upper curves is 1 dB higher than for the lower curves. The amplitude curve is in both cases quite noisy and contains no clear evidence for unusual behavior. Several bias frequencies were tried; however, the phase curves have very clear anomalies. In the top trace there are indications for an instability for every other flux quantum. In the bottom trace the instability occurs for every flux quantum. Notice that the phase jumps are at the maximum of the signal. Thus, they are unlikely to be associated with flux noise (if there was no instability, the flux-to-signal transfer coefficient would be low in the neighborhood of the maximum, where the derivative is small; rather, noise-induced spikes would be expected where the slope is large, i.e., away from the maximum). Indeed the signal maxima are where the instability is expected to show up according to the model.⁵

IV. CONCLUSIONS

An experimental study of the signal characteristics of a ceramic YBCO rf SQUID operated at 77 K has been carried out. Both amplitude and phase detection have been used. A low critical current of the ceramic weak link places the SQUID in the inductance mode regime, where the main effect of the SQUID loop is to act as a parametric inductance resulting in frequency shifts of the tank-circuit resonance. The frequency shifts have been directly ob-

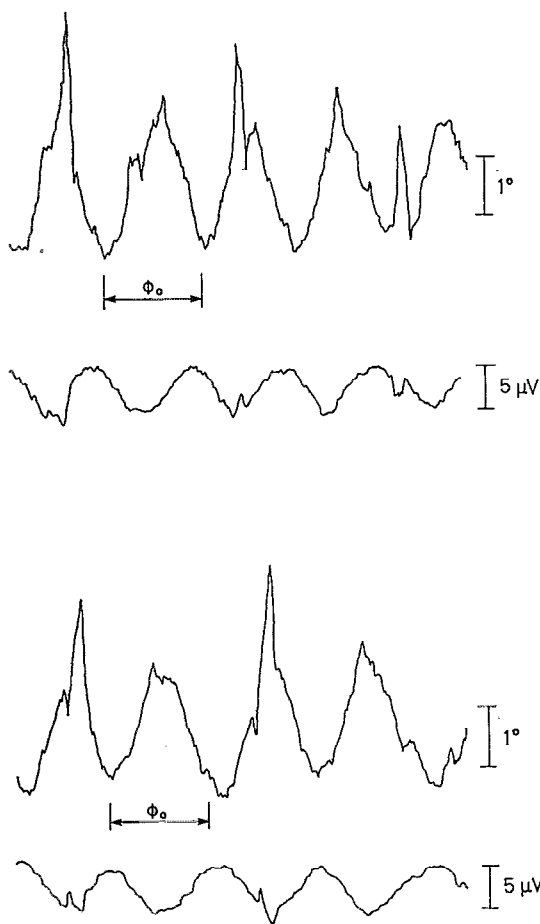


FIG. 6. Examples of instabilities in the SQUID signals. Phase and amplitude variations simultaneous recorded are shown. $f_{\text{bias}}=28.5$ MHz, $\phi_{\text{rf}}\approx 5\Phi_0$, but the top curves are obtained with a pumping level 1 dB over that of the bottom curves.

served with changing bias current. Some dissipation is also observed to take place, so the SQUID is not in the clean inductance mode limit, but rather near the $\beta=1$ crossover between inductance mode and hysteretic (dissipative mode). The experimental results have been qualitatively compared with a model in the $\beta\ll 1$ limit. The model is based on the RSJ model for the weak link. The main features of the model predictions are found in the data, although a detailed, qualitative comparison is not possible. Still the comparison bears some evidence that the RSJ model is reasonable to use, even for the extended (20–30 μm) weak link in the ceramic.

In particular, the instabilities predicted by the theory were clearly observed. The enhancement of the transfer coefficients in the vicinity of the instability can in principle be used to increase the SQUID sensitivity and make it comparable to that of dc SQUIDs. However, this will require operation in a flux-locked mode with electronics which presumably must be more complicated than usually employed.

For the present SQUID the tank-circuit noise will dominate in any case as argued in the following. Only the fundamental thermal noise is considered. In the inductance mode the tank-circuit noise will dominate if $k^2 Q \beta \omega / \omega_J < T_K / T$, where ω is the bias frequency and ω_J is the Josephson frequency of the weak link. T_K is the tank-circuit temperature and T is the SQUID temperature.⁵ In our case $T_K > \approx T$, and $Q \approx 30$, while $\omega_J / 2\pi$ may be estimated to 10 GHz ($\omega_J = 2\pi R_N I_C / \Phi_0$, where R_N is the normal resistance, and $R_N I_C$ for a ceramic junction typically is 10–50 μV). The quantity $k^2 \beta$ can be estimated experimentally from⁵ $k^2 \beta \approx a(\omega_1 - \omega_2) / [2\omega_p J_1(a)]$, where $a = 2\pi \phi_{\text{rf}} / \Phi_0$, and ω_1 and ω_2 are the resonance frequencies corresponding to $\phi_{\text{rf}} = \Phi_0 / 2$, and $\phi_{\text{rf}} = \Phi_0$, respectively. ω_p is the resonance frequency for high pumping power ($\phi_{\text{rf}} \gg \Phi_0$), while J_1 is the Bessel function of the first kind. This leads to $k^2 \beta \approx 0.12$ and therefore $k^2 Q \beta \approx 4$. Since $\omega / \omega_J \approx 3 \times 10^{-3}$, the condition above is cleanly fulfilled. To make the tank-circuit noise less than the noise from the interferometer (SQUID) would require both increasing the quality factor Q and the bias frequency ω . These considerations provide guidelines for any further attempts to put the inductance mode instabilities into practical use.

ACKNOWLEDGMENTS

We would like to thank V. V. Kuttyrev, J. Mygind, and A. Kühle for advice on the experiments as well as for useful discussions of the results.

¹V. M. Zakosarenko, E. V. Il'ichev, and V. A. Tulin, JETP Lett. **51**, 315 (1990) [transl. from Pis'ma Zh. Eksp. Teor. Fiz. **51**, 275 (1990)].

²Y. Zhang, H.-M. Müick, K. Herrmann, J. Schubert, W. Zander, A. I. Braginski, and C. Heiden, Appl. Phys. Lett. **60**, 645 (1992); Y. Zhang, H.-M. Müick, M. Bode, K. Herrmann, J. Schubert, W. Zandez, A. J. Braginski, and C. Heiden, *ibid.* **60**, 2303 (1992).

³See, for example, B. Oh, R. H. Koch, W. J. Gallagher, R. P. Robertazzi, and W. Eidelloth, Appl. Phys. Lett. **59**, 123 (1991).

⁴A. Barone and G. Paterno, *Physics and Applications of the Josephson Effect* (Wiley, New York, 1982).

⁵K. K. Likhavov and B. T. Ulrich, *Systems with Josephson Junctions* (Moscow University Press, Moscow, 1978) (in Russian).

⁶I. M. Dmitrenko, G. M. Tsoi, V. I. Shnyrkov, and V. V. Kartsovnik, J. Low-Temp. Phys. **49**, 417 (1982).